The Hop Cassette of the PAC1 Receptor Confers Coupling to Ca^{2+} Elevation Required for Pituitary Adenylate Cyclase-activating Polypeptide-evoked Neurosecretion*

Tomris Mustafa[‡1], **Maurizio Grimaldi**[‡§], and **Lee E. Eiden**[‡2]

From the ‡Section on Molecular Neuroscience, Laboratory of Cellular and Molecular Regulation, National Institute of Mental Health, Bethesda, Maryland 20892 and the §Laboratory of Neuropharmacology, Department of Biochemistry, Drug Discovery Division, Southern Research Institute, Birmingham, Alabama 35205

We have identified the single PAC1 receptor variant responsible for Ca^{2+} mobilization from intracellular stores and influx through voltage-gated Ca^{2+} channels in bovine chromaffin cells and the domain of this receptor variant that confers coupling to $[Ca^{2+}]_i$ elevation. This receptor ($bPAC1_{hop}$) contains a 28-amino acid "hop" insertion in the third intracellular loop, with a full-length 171-amino acid N terminus. Expression of the $bPAC1_{hop}$ receptor in NG108-15 cells, which lack endogenous PAC1 receptors, reconstituted high affinity PACAP binding and PACAP-dependent elevation of both cAMP and intracellular Ca^{2+} concentrations ($[Ca^{2+}]_i$). Removal of the hop domain and expression of this receptor ($bPAC1_{null}$) in NG108-15 cells reconstituted high affinity PACAP binding and PACAP-dependent cAMP generation but without a corresponding $[Ca^{2+}]_i$ elevation. PC12-G cells express sufficient levels of PAC1 receptors to provide PACAP-saturable coupling to adenylate cyclase and to drive PACAP-dependent differentiation but do not express PAC1 receptors at levels found in postmitotic neuronal and endocrine cells and do not support PACAP-mediated neurosecretion. Expression of $bPAC1_{hop}$, but not $bPAC1_{null}$, at levels comparable with those of $bPAC1_{hop}$ in bovine chromaffin cells resulted in acquisition by PC12-G cells of PACAP-dependent $[Ca^{2+}]_i$ increase and extracellular Ca^{2+} influx. In addition, PC12-G cells expressing $bPAC1_{hop}$ acquired the ability to release [³H]norepinephrine in a Ca^{2+} influx-dependent manner in response to PACAP. Expression of PACAP receptors in neuroendocrine rather than nonneuroendocrine cells reveals key differences between $PAC1_{hop}$ and $PAC1_{null}$ coupling, indicating an important and previously unrecognized role of the hop cassette in PAC1-mediated Ca^{2+} signaling in neuroendocrine cells.

Pituitary adenylate cyclase-activating polypeptide (PACAP)[3] stimulates hormone secretion from adrenomedullary chromaf-

fin cells in culture and *in vivo* (1–8). PACAP also increases the biosynthesis of catecholamines (9, 10) and neuropeptides, such as Met-enkephalin (2, 11), and VIP (8, 12) required to replenish hormone stores and sustain long term secretion. Thus, PACAP is an important slow transmitter at the adrenomedullary synapse that stimulates catecholamine and neuropeptide release and maintains adequate levels of hormones for the prolonged secretion associated with sustained metabolic or psychogenic stress (13–15). PACAP fulfills a similar function at postganglionic sympathetic synapses, enhancing the expression as well as the release of neuropeptides through engagement of multiple signaling pathways, including inositol trisphosphate (IP_3) and cAMP (16–19).

The actions of PACAP in the sympathoadrenal axis are mediated mainly through its G-protein-coupled receptor, PAC1. Several PAC1 variants exist in neurons and endocrine cells, which differ at the N terminus and in the third intracellular loop (IC3) of this G-protein-coupled receptor (GPCR). N-terminal splice variants show slightly different affinities for PACAP binding but similar G-protein-coupling properties (20, 21). IC3 variants originate from the alternative splicing of neither, one, or both of two exons, hip or hop, within this region (22, 23). All variants, including $PAC1_{null}$, which has neither hop nor hip insertions in IC3, bind PACAP-38 and PACAP-27 with high affinity and couple to G_s to activate adenylate cyclase (AC) (22, 23). Insertion of the hip cassette in the PAC1 receptor either abolishes or impairs coupling to phospholipase C (PLC) when these receptors are expressed in the nonneuroendocrine LLC-PK1 (LLC-PK1, pig kidney epithelial) or NIH3T3 (mouse embryonic fibroblast) cell lines (22, 23). Human $PAC1_{hop}$ and $PAC1_{null}$ receptors couple to both AC and PLC in the Chinese hamster ovary cell line (CHO) commonly used for receptor reconstitution; however, $PAC1_{hop}$ uniquely binds to other signaling molecules, at least in these cells, that could explain differential signaling between the two receptor variants (24, 25). Finally, a rat PAC1 variant consisting of an amino acid substitution in transmembrane region two and a two-amino acid deletion with a two-amino acid substitution in transmembrane

region four has been reported to mediate Ca^{2+} influx in CHO cells, without coupling to AC (26), although the existence of this variant in other species is in doubt (14). Thus, the structural basis for PAC1 receptor coupling to cytosolic Ca^{2+} mobilization and extracellular influx in neuronal and endocrine cells remains unresolved, significantly impeding progress in understanding this crucial aspect of class II GPCR-Ca^{2+} coupling.

Determining receptor variant specificity unambiguously with respect to second messenger coupling is key to understanding the mechanisms of PACAP-evoked exocytosis, since stimulation of exocytosis by PACAP and other neurotransmitters may be modulated by cAMP and interactions between cAMP and Ca^{2+} in addition to the required rise in cytosolic Ca^{2+} concentration ([Ca^{2+}]$_i$) that triggers the final step of exocytosis (27). PACAP-mediated secretion from bovine chromaffin cells (BCCs) and rat pheochromocytoma (PC12) cells is reported to require Ca^{2+} influx through voltage-gated Ca^{2+} channels (VGCCs), with predominant contributions from either L-type or non-L-type channels depending on the time frame of secretion and the type of cell (1, 2, 5, 8, 28, 29). Since all PAC1 receptor variants elevate cAMP, various laboratories have investigated cAMP involvement in potentiating PACAP-induced [Ca^{2+}]$_i$ elevation or otherwise contributing to PACAP-induced secretion from chromaffin cells (30–33). PACAP also causes depolarization of pituitary cells, pinealocytes, and sympathetic neurons through Na$^+$ channels or Ca^{2+} influx through nonspecific cation or transient receptor potential channels (17, 34–36), pathways that may also contribute to Ca^{2+} influx required for exocytosis.

PAC1 receptor activation could therefore stimulate secretion both directly and indirectly through Ca^{2+} mobilization from intracellular stores, Ca^{2+} influx, and cAMP generation. Evidence for PACAP coupling to these second messengers through PAC1 comes from a variety of endocrine and nonendocrine cells, however, and may be specific to both the cell type and receptor variant. Therefore, identifying the mechanism of secretion triggered by PACAP at the adrenomedullary synapse, at which PACAP is the major physiologically relevant slow transmitter, requires (*a*) identification of the PAC1 variant or variants present in chromaffin cells, (*b*) reconstitution of PACAP-dependent calcium signaling and secretory competence in a neuroendocrine cell background, and (*c*) determination of the structural motifs responsible for reconstituted signaling leading to secretion. We demonstrate here that BCCs express a single PACAP receptor, bPAC1$_{hop}$, and reveal the structural requirements for coupling to intracellular Ca^{2+} mobilization, Ca^{2+} influx, and neurosecretion through reconstitution in PC12-G cells.

EXPERIMENTAL PROCEDURES

Materials—PACAP-38 and PACAP-27 were purchased from Phoenix Pharmaceuticals (Mountain View, CA). The radioligand, [^{125}I]PACAP-27 (specific activity 2200 Ci/mmol) was obtained from PerkinElmer Life Sciences. Tetrodotoxin (TTX), veratridine, and forskolin were purchased from Calbiochem-EMD Biosciences. All tissue culture reagents were purchased from Invitrogen unless otherwise specified. All other reagents used were purchased from Sigma-Aldrich.

Chromaffin Cell Cultures—Steer adrenal glands were used to isolate chromaffin cells as previously described (37, 38). Freshly isolated chromaffin cells were seeded into 162-cm^2 tissue culture flasks and cultured for 24 h in high glucose Dulbecco's modified Eagle's medium (DMEM) supplemented with 5% heat-inactivated fetal calf serum, 25 mM HEPES, 100 units/ml penicillin/streptomycin, 2 mM glutamine, 10 μg/ml cytosine β-D-arabinofuranoside (chromaffin cell complete medium; CCCM) with 100 units/ml nystatin prior to differential plating into 24-well plates. For radioimmunoassays, chromaffin cells were replated at a density of 500,000 cells/well on 0.1 mg/ml poly-D-lysine-coated 24-well plates (Costar-Corning) 24 h prior to treatments or harvesting.

Measurement of Met-Enkephalin Release—Release studies were performed on chromaffin cells 24 h after differential plating. Briefly, cells were pretreated for 30 min with 500 μl of CCCM containing 30 μM D600, 1 μM TTX, 10 μM nimodipine, vehicle, or Ca^{2+}-free CCCM (Ca^{2+} concentration from serum alone, ~100 μM). A further 500 μl of CCCM or Ca^{2+}-free CCCM, either with or without 200 nM PACAP-38 or 20 μM veratridine, was then added to each well containing each of the above inhibitors, resulting in a final concentration of 100 nM PACAP or 10 μM veratridine/1000-μl final well volume. Following 1 h of treatment, Met-enkephalin was assayed from medium aliquots or 0.1 N HCl-lyophilized cell extracts by radioimmunoassay (37). The statistical difference between control and treatment groups was determined using one-way analysis of variance by Tukey's multiple comparison test using GRAPHPAD PRISM, version 4 (GraphPad Software).

Preparation of cDNA—Bovine chromaffin, NG108-15, or PC12-G cells grown in Costar 162-cm^2 flasks (Corning) were harvested, washed once with phosphate-buffered saline, rapidly resuspended in Trizol (Invitrogen), snap-frozen, and stored at −80 °C. Total RNA was then isolated using the RNeasy® Mini total RNA isolation kit (Qiagen) according to the manufacturer's instructions with the following modifications. Samples were thawed on ice and extracted with a final concentration of 20% chloroform. Following centrifugation at 10,000 rpm for 10 min at 4 °C, an equal volume of 70% ethanol was added to the aqueous phase, and the sample was applied to the RNeasy® Mini spin column and processed according to Ref. 69. First strand cDNA was synthesized from 5 μg of total RNA using the Superscript™ First-Strand Synthesis System according to the manufacturer's instructions (Invitrogen). Reverse transcription-PCR reactions were carried out using 1 μl (~250 ng) of the first-strand cDNA synthesis reaction as described below.

Identification and Cloning of the BCC PAC1 Receptor—The previously published sequence of the cloned bovine brain PAC1 receptor (accession number D17290) (39) was used to design a series of primers to amplify the receptor in overlapping segments and test for splice variants as described in Fig. 3. Primers (5′-ATGAGAGGCGGGCGGCACTG-3′ and 5′-CCAACTG-TGTACAGGGCCTTCACTG-3′) were used to isolate the N-terminal region of the PAC1 receptor. The entire transmembrane 1–7 region, including the third intracellular loop known to contain inserts, was amplified using primers (5′-GCCCTG-TACACAGTTGGCTACA-3′ and 5′-TTGATCTCCGCCTG-CACCTC-3′). The C terminus of the receptor was finally ampli-

fied using primers (5′-AGAGGTGCAGGCGGAGATCA-3′ and 5′-TCAGGTGGCCAGGTTGTCGG-3′), resulting in the generation of three overlapping amplicons representing the full-length PAC1 receptor. To further investigate the presence of third intracellular loop variants containing either hip, hop, or hiphop cassette insertions, transmembrane region 5–6 was amplified with primers (5′-GGCCCTGTAGTTGGCTC-CATAATGG-3′ and 5′-GGGAGAAAGCAAAGACAGTG-3′). To determine which cassette was present in the IC3 region located between TM regions 5 and 6, the TM5 forward primer (5′-GGCCCTGTAGTTGGCTCCATAATGG-3′) was used in combination with reverse primers designed to anneal within the bovine hop (5′-AGAGTAATGGTGGACAGTTCTGACA-3′) or rat hip (5′-AGGAAAGGGGGTGAATGCTG-3′) cassettes. All PCRs contained a 0.25 μM concentration of each primer, 1 mM dNTPs, 5 mM MgCl$_2$, 2.5 units of high fidelity *Pfu* Turbo DNA polymerase (Stratagene), and ~250 ng of cDNA template. Amplification consisted of an initial denaturation step of 95 °C for 5 min followed by 36 cycles of 95 °C for 30 s, 65 °C for 1 min, 72 °C for 1 min with a final extension step of 72 °C for 10 min.

The entire open reading frame of the bovine PAC1 receptor was obtained using primers (5′-ATGAGAGGCGGGCG-GCACTG-3′ and 5′-TCAGGTGGCCAGGTTGTCGG-3′) under the PCR conditions specified above. The amplified bovine chromaffin PAC1 receptor cDNA was then directly cloned into the pCR®II-TOPO plasmid (Invitrogen) according to the manufacturer's instructions. Recombinant plasmids containing the entire open reading frame (ORF) or various segments of the receptor were sequenced using M13 reverse and M13 forward primers by the dideoxy chain termination method (DNA Sequencing Facility, NINDS, National Institutes of Health). Following multiple sequence verification, the bovine chromaffin cell PAC1 receptor cDNA was subcloned into a mammalian expression vector, pcDNA3, and used for all subsequent studies.

Removal of the Hop Cassette—The entire hop cassette was removed from the bovine PAC1 receptor using PCR-mediated deletion mutagenesis based on a previously described method (40, 41). Briefly, first round PCR was carried out using one chimeric and one nonchimeric primer to amplify the upstream and downstream regions immediately surrounding the hop cassette to be deleted. The PCR amplicons were then diluted 1:1000, and 1 μl of the upstream and downstream amplicons were combined and used as template for a second round of ligation PCR using the outermost primer pairs (forward primer, 5′-TGAAT-GAGAGGCGGGCGGCA-3′; reverse primer, 5-GGCTCAG-GTGGCCAGGTTGT-3′). PCRs were carried out according to the conditions described above. The final single amplicon was purified and cloned into pcDNA3, and deletion of the hop cassette was confirmed through multiple sequencing reactions.

Cell Culture—NG108-15 cells (rat neuroblastoma × mouse glioma) obtained from the American Type Culture Collection (Manassas, VA) were cultured in high glucose DMEM supplemented with 10% heat-inactivated fetal calf serum (Hyclone), 100 units/ml penicillin/streptomycin, 2 mM glutamine, and 1× HAT (sodium hypoxanthine, aminopterin, and thymidine) supplement. PC12-G rat pheochromocytoma cells (42) were cultured in high glucose DMEM supplemented with 7% heat-inactivated fetal calf serum (Hyclone), 7% horse serum (Bio-Whittaker-Cambrex, Walkersville, MD), 25 mM HEPES, 100 units/ml penicillin/streptomycin, and 2 mM L-glutamine. All cells were used between passages 6 and 30.

Stable and Transient Transfection Studies—NG108-15 cells were transfected (24-well plate, 2-cm^2 surface area) with a mixture of 0.8 μg of DNA (pcDNA3 alone; pcDNA3 containing the bovine PAC1 receptor (bPAC1$_{hop}$) cDNA; pcDNA3 containing the bovine PAC1 receptor deletion mutant (bPAC1$_{null}$) cDNA; or pRT43.2, a cytomegalovirus promoter-driven GFP reporter plasmid, and 2 μl of Lipofectamine™ (Invitrogen) in the absence of serum according to the manufacturer's instructions). For creation of bPAC1$_{hop}$ stable cell lines, NG108-15 cells were transfected with PvuI (New England Biolabs)-linearized pcDNA3 containing bPAC1$_{hop}$ receptor cDNA as described above. Cells were then selected using 500 μg/ml G418 and continuously maintained in 300 μg/ml G418 thereafter. Stable cell lines were screened through receptor binding studies and selected based on their ability to bind [^{125}I]PACAP-27 compared with mock-transfected NG108-15 cells. PC12-G cells were transfected (24-well plate, 2-cm^2 surface area) with 1 μg of DNA as specified above and 2 μl of Lipofectamine2000™ (Invitrogen) in the presence of serum according to the manufacturer's instructions. For creation of stable cell lines, PC12-G cells were transfected with linearized plasmid as described above and selected and continuously maintained using 500 μg/ml G418. PC12-G cells stably expressing the bPAC1$_{hop}$ receptor were selected based on gain of [^{125}I]PACAP-27 binding and Ca^{2+} mobilization compared with mock-transfected naive PC12-G cells. All transiently transfected cells were assayed 48 h post-transfection, whereas stable cell lines were plated 24 h prior to experimentation.

Preparation of Crude Cell Membranes—Crude membranes were prepared as previously described (43). Briefly, subconfluent cells were harvested in hypotonic buffer (50 mM Tris-HCl and 5 mM EDTA, pH 7.4), homogenized with a hand-held tissue homogenizer (Tissuemizer; Fisher Scientific) for 10 s, and centrifuged at 600 × g for 5 min to remove cellular debris. The supernatant was centrifuged at 25,000 rpm for 20 min, and the membrane pellet was resuspended in PACAP wash buffer (50 mM Tris-HCl, 5 mM MgCl$_2$, pH 7.4) supplemented with Roche cocktail inhibitor tablets (Roche Applied Science). Total protein concentration was determined using the Bio-Rad DC protein colorimetric assay according to the manufacturer's instructions (Bio-Rad).

Receptor Binding Studies—NG108-15 or PC12-G cell membranes (30 μg) were incubated in the presence of 150 pM [^{125}I]PACAP-27 and increasing concentrations of unlabeled PACAP-38, PACAP-27, and VIP in PACAP binding buffer (50 mM Tris-HCl, 5 mM MgCl$_2$, pH 7.4) supplemented with 0.5 mg/ml bacitracin, 200 μM phenylmethylsulfonyl fluoride, 100 μM aprotinin, and 1% bovine serum albumin) for 1.5 h at 37 °C. All assays were set up and incubated in Multiscreen™ glass fiber plates (Millipore), precoated for 2 h at 4 °C with 0.1% polyethyleneimine prepared in PACAP wash buffer as described above. Free and bound radioligand were then separated by filtration using the multiscreen vacuum manifold according to

the manufacturer's instructions. Plates were washed four times with ice-cold PACAP wash buffer, filters were punched, and the retained radioactivity was measured on a γ-counter. The radioligand binding data were analyzed using version 4 of the GRAPHPAD PRISM program.

Intracellular cAMP Measurements—Stably transfected NG108-15 cells were plated onto 24-well plates (Costar-Corning) coated with poly-L-lysine (0.1 mg/ml in phosphate-buffered saline) at a density of 70,000 cells/well 24 h prior to being serum-deprived for 24 h. For transient transfection studies, cells were plated at a density of 70,000 cells/well 24 h post-transfection according to the conditions described above and serum-deprived 24 h prior to treatments. The NG108-15 cells were then treated with varying concentrations (10^{-7} to 10^{-11} M) of PACAP-38, PACAP-27, or VIP for 20 min at 37 °C in DMEM containing 100 units/ml penicillin/streptomycin, 2 mM glutamine, 1× HAT supplement, 1 mM isobutylmethylxanthine, and 0.1% bovine serum albumin. Intracellular cAMP was then measured using the Biotrak nonacetylation enzyme immunoassay system with the supplied lysis reagent according to manufacturer's instructions (Amersham Biosciences). 24 h post-transfection, PC12-G cells were plated into 24-well plates coated with 0.1 mg/ml poly-L-lysine at a density of 250,000 cells/well, allowed to adhere for 24 h, and then treated with varying concentrations (10^{-7} to 10^{-11} M) of PACAP-38, PACAP-27, or VIP for 20 min at 37 °C. Intracellular cAMP content was determined as described above.

Single Cell [Ca²⁺]ᵢ Measurements—$[Ca^{2+}]_i$ was measured as previously described (44). Briefly, 150,000 (NG108-15) or 400,000 (PC12-G) cells were seeded onto 1.5-cm diameter glass coverslips (Assistent) coated with 0.5 mg/ml poly-L-lysine in 12-well plates (Costar-Corning). Transiently transfected cells were plated 24 h post-transfection at the cell densities specified above. For transient transfection studies, cells were co-transfected at a ratio of 1:3 (bPAC1$_{hop}$ or bPAC1$_{null}$ in pcDNA3:pRT43.2GFP) in 162-cm² flasks and plated 24 h post-transfection under the specified conditions. 24 h postseeding, cells were washed once with Krebs-Ringer buffer (KRB) containing 125 mM NaCl, 5 mM KCl, 1 mM Na₂HPO₄, 1 mM MgSO₄, 1 mM CaCl₂, 5.5 mM glucose, and 20 mM HEPES, pH 7.3. The cells were then loaded with 4 μM Fura-2/AM (Invitrogen) in KRB for 22 min at room temperature. Following loading, cells were washed once with KRB and incubated for a further 22 min at room temperature in Fura-2/AM-free KRB. The coverslips were then mounted onto a custom-built perfusion chamber and placed on an inverted Olympus microscope equipped with a 40× high numerical aperture 340-nm optimized lens and perfused with KRB in the presence or absence of drugs. Ca²⁺-free studies were carried out as described above using Ca²⁺-free KRB supplemented with 100 μM EGTA. The preparations were then excited at 340 and 380 nm, respectively, and fluorescence intensity was measured every 2 s at an emission wavelength of 510 nm. Images were digitally captured and analyzed with the software MetaFluor (Molecular Devices). Among transiently transfected cells, bPAC1$_{hop}$- or bPAC1$_{null}$- expressing cells were identified by GFP fluorescence prior to $[Ca^{2+}]_i$ measurements, compared with GFP-nonexpressing, untransfected NG108-15 or PC12-G cells. Ratio values were

then converted to calibrated $[Ca^{2+}]_i$ values. F_{max} values were obtained by exposing the cells to 10 μM ionomycin in 1 mM Ca²⁺-containing KRB, and F_{min} values were obtained by exposing ionomycin-treated cells to Ca²⁺-free KRB supplemented with 100 μM EGTA. The corresponding ratios, F_{min} and F_{max} were substituted into the equation described by Grynckiewicz *et al.* (45) to convert data point ratios to $[Ca^{2+}]_i$. Individual calibrations were used for each cell type analyzed in this study.

Catecholamine Uptake and Release Assay—Naive PC12-G cells or PC12-G cells stably expressing the bPAC1$_{hop}$ receptor were plated at a density of 200,000 cells/well in 0.1 mg/ml poly-L-lysine-coated 24-well plates and allowed to adhere for 24 h. Cells were labeled with 1 μCi/well levo-[7-³H]norepinephrine (1 mCi/ml; PerkinElmer Life Sciences) in PC12 complete media for 4 h at 37 °C. For treatments, cells were washed once with phosphate-buffered saline and preincubated for 30 min at 37 °C in 400 μl of KRB as described above. Cells were subsequently stimulated by the addition of 100 μl of KRB with or without 5× concentrated secretagogues, resulting in a final concentration of 100 nM PACAP-38 or 55 mM KCl. Following stimulation for 30 min at 37 °C, the total medium (500 μl) was collected, and cells were lysed with 500 μl of KRB containing 1% Triton X-100. Ca²⁺-free studies were carried out using Ca²⁺-free KRB supplemented with 100 μM EGTA as described above. The level of radioactivity in both medium and cell lysates was then determined by liquid scintillation counting. Levo-[7-³H]norepinephrine secretion was calculated as the percentage of total radioactivity released, where total activity is the amount released plus the amount remaining in the cells. The statistical difference between control and treatment groups was determined using one-way analysis of variance by Tukey's multiple comparison tests using GRAPHPAD PRISM, version 4.

RESULTS

Characteristics of PACAP-stimulated Neuropeptide Secretion and [Ca²⁺]ᵢ Elevation in BCCs—We examined the Ca²⁺- and cAMP-dependent characteristics of PACAP-regulated acute (1-h) secretion from bovine chromaffin cells using endogenous Met-enkephalin as a marker of release from large dense core vesicles (46). The ability of PACAP to cause Met-enkephalin release from BCCs was not dependent on Na⁺ influx-evoked cellular depolarization, since TTX, which inhibits voltage-dependent Na⁺ influx leading to action potential generation and opening of VGCCs, failed to block PACAP-evoked secretion (Fig. 1). Treatment of cells with 25 μM forskolin did not mimic the acute secretagogue effects of PACAP under conditions (Met-enkephalin secretion during 60 min of stimulation) in which 40 mM KCl or 100 nM PACAP gave a 3–5-fold stimulation over basal level (data not shown), indicating that the ability of PACAP to elevate intracellular cAMP by coupling to adenylate cyclase through Gα$_s$ is insufficient on its own to stimulate acute secretion from large dense core vesicles in BCCs. PACAP-evoked secretion of Met-enkephalin was abolished in Ca²⁺-free medium (Fig. 1) and by exposure of BCCs to 30 μM D600, a pan-specific inhibitor of VGCCs (Fig. 1), consistent with previous reports that PACAP-dependent Ca²⁺ influx occurs through one or more VGCCs in BCCs (1, 36). Blockade of PACAP-evoked acute secretion, unlike regulation of neu-
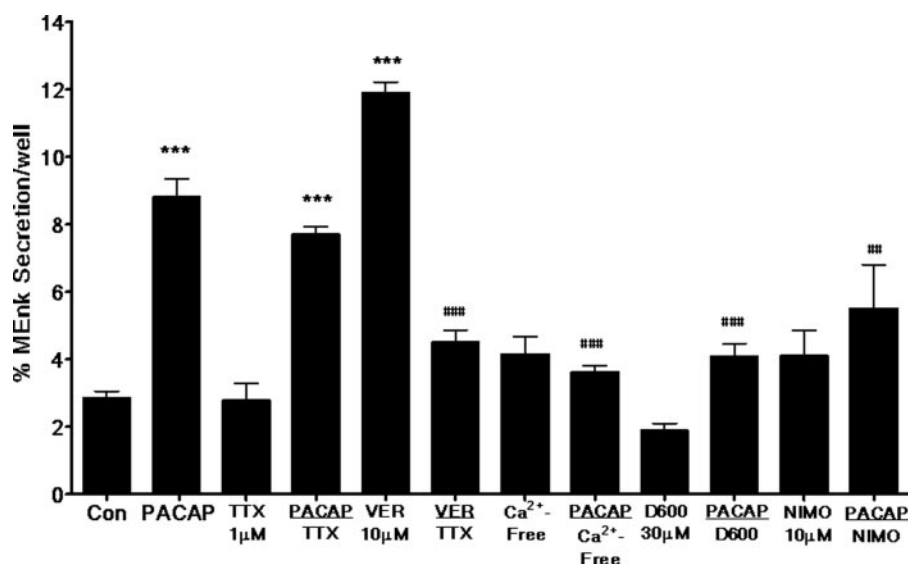
FIGURE 1. **PACAP-mediated Met-enkephalin secretion from BCCs is dependent on Ca²⁺ influx.** Met-enkephalin secretion elicited by 100 nM PACAP is not blocked by 1 μM tetrodotoxin (*TTX*), whereas TTX blocks 10 μM veratridine (*Ver*)-evoked secretion. PACAP-evoked Met-enkephalin secretion is Ca²⁺ influx-dependent and can be abolished in the absence of extracellular Ca²⁺. PACAP-evoked extracellular influx occurs through VGCCs as indicated by the ability of 30 μM D600 to inhibit PACAP-evoked secretion. Nimodipine, an inhibitor of L-type VGCCs, significantly blocks PACAP-evoked Met-enkephalin secretion in BCCs. Values are the mean ± S.E. of triplicate wells. Each experiment was repeated at least two times with similar results. Differences between control and treatment groups were determined using one-way analysis of variance followed by *post hoc* Tukey's multiple comparison test. ***, $p < 0.0001$; **, $p < 0.001$ compared with corresponding control. ###, $p < 0.0001$; ##, $p < 0.001$ compared with corresponding treatment.

ropeptide biosynthesis and sustained (24–72-h) secretion (2, 8), was also blocked by the L-type Ca²⁺ channel inhibitors, nimodipine (Fig. 1) or 10 μM (−)-202–791 (data not shown).

Exposure of chromaffin cells (resting 70 ± 2.09 nM $[Ca^{2+}]_i$) to PACAP results in a large elevation of $[Ca^{2+}]_i$ that is characterized by a fast and large peak (516 ± 55 nM $[Ca^{2+}]_i$), followed by a plateau phase (272 ± 19 nM $[Ca^{2+}]_i$) (Fig. 2*A*; see Ref. 8), corresponding to PACAP-evoked acute secretion. Consistent with our secretion studies, the presence of 1 μM TTX did not block PACAP-induced $[Ca^{2+}]_i$ elevation (Fig. 2*B*) (PACAP + TTX peak, 2100 ± 335 nM $[Ca^{2+}]_i$), confirming that the effects of PACAP on $[Ca^{2+}]_i$ do not occur through voltage-dependent Na⁺ channel-mediated membrane depolarization. In the absence of extracellular Ca²⁺, PACAP still caused a transient increase of $[Ca^{2+}]_i$ (143 ± 19 nM $[Ca^{2+}]_i$), which rapidly returned to base-line levels (Fig. 2*C*), showing that the effect of PACAP on $[Ca^{2+}]_i$ occurs through both Ca²⁺ mobilization from ICS and extracellular influx. This was confirmed by complete abolition of $[Ca^{2+}]_i$ elevation when BCC ICS were depleted by thapsigargin prior to PACAP treatment in the presence of nimodipine, an inhibitor of L-type VGCCs (Fig. 2*D*) (resting, 58 ± 7 nM; Nimo base line, 73 ± 4.2 nM; Thap + Nimo, 211 ± 20 nM; PACAP + Nimo + Thap, 85 ± 5 nM $[Ca^{2+}]_i$).

BCCs Express a Single Isoform of the PAC1 Receptor—We next examined the molecular forms of the PAC1 receptor(s) responsible for PACAP-mediated $[Ca^{2+}]_i$ elevation and secretion in BCCs. The PAC1 receptor variant(s) expressed by BCCs was identified and cloned using the previously published sequence of the bovine brain PAC1 receptor (accession number D17290) (39) to design a set of primers to amplify the entire open reading frame (ORF) of the receptor in three overlapping

segments: the N terminus, transmembrane regions 1–7, and the C terminus (Fig. 3). First, amplification of the N terminus region indicated the presence of a full-length transcript without the 21- or 57-amino acid truncations reported in some PAC1 transcripts (20, 21) or insertion of 24 amino acids reported in others (47). Generation of an 857-bp transcript following amplification of the TM1 to -7 region of the receptor could be accounted for only by the presence of a single hip or hop cassette, but not both, in the third intracellular loop of the receptor (22, 48). The use of internal primers to the hop or hip cassettes confirmed that the bovine PAC1 receptor contained the hop cassette within its IC3 region.

Importantly, the hop variant was the only PAC1 receptor species present in BCCs (Fig. 3*B*). No C terminus receptor variants of the PAC1 receptor were identified in bovine chromaffin cells, as shown by the single amplicon of the expected length of 193 bp in Fig. 3*B*. Following multiple sequence verifications, our results indicated that BCCs express a single splice variant of the receptor with the hop cassette in the IC3 loop. Finally, multiple sequencing of amplicons encompassing the fourth transmembrane domain failed to identify the reported transmembrane variant responsible for PAC1 receptor coupling to Ca²⁺ influx reported previously (26), consistent with the absence of this sequence in either the human or rodent *PAC1* gene loci (14). Since it is the only form of the PAC1 receptor expressed in bovine chromaffin cells, bPAC1$_{hop}$ can be identified unambiguously with PACAP coupling to both cAMP generation and Ca²⁺ mobilization and influx in these cells. This receptor was next expressed in homologous (neural and neuroendocrine) cells to recapitulate PACAP-dependent Ca²⁺ signaling required for secretion.

Expression of the bPAC1$_{hop}$ Receptor in NG108-15 Cells Reconstitutes High Affinity PACAP Binding, PACAP-stimulated cAMP Generation, and Elevation of $[Ca^{2+}]_i$—bPAC1$_{hop}$ was expressed in NG108-15 cells, a mouse neuroblastoma × rat glioma cell line, which lacks endogenous expression of either PACAP or VIP receptors but is capable of GPCR-mediated responses to other neurotransmitters (49). [¹²⁵I]PACAP-27 binding was specifically competed by unlabeled PACAP-38 and PACAP-27 with IC₅₀ values of 3 and 18 nM, respectively, and VIP did not compete for [¹²⁵I]PACAP-27 binding (Fig. 4*A*). Both PACAP-38 and PACAP-27 stimulated the accumulation of intracellular cAMP in a concentration-dependent manner, with EC₅₀ values of 0.14 and 0.05 nM, respectively, in NG108-15 cells stably transfected with bPAC1$_{hop}$, indicating that coupling
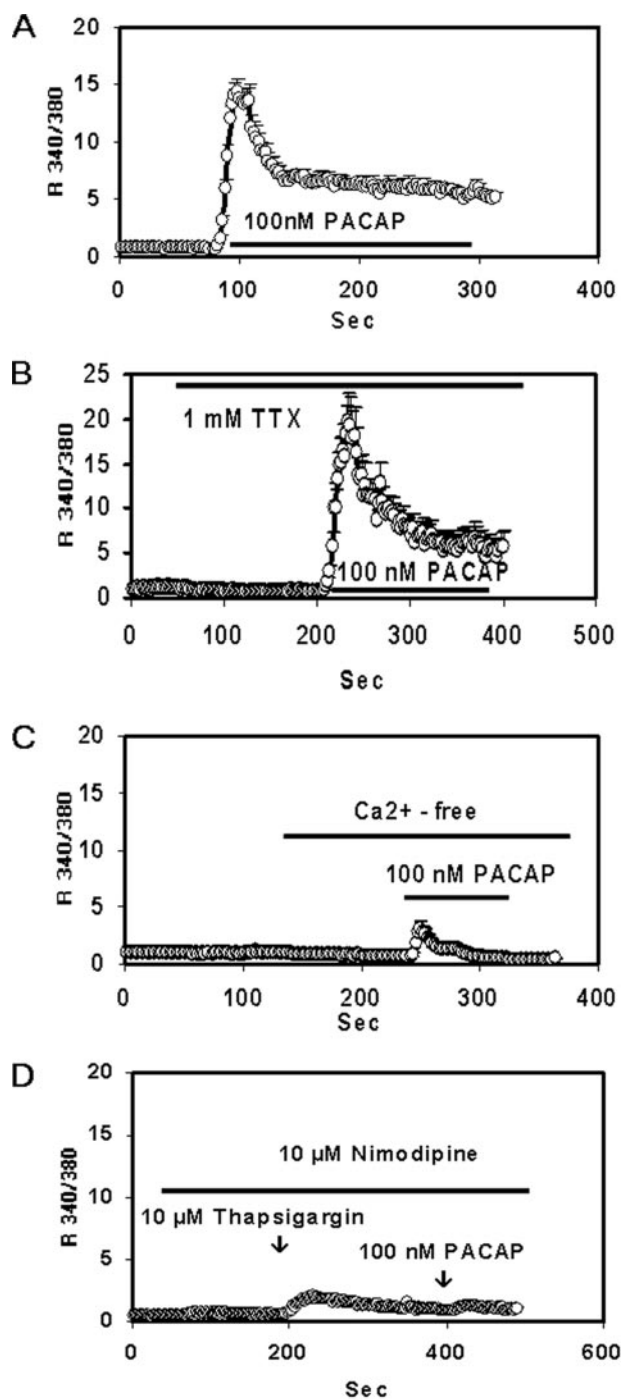
FIGURE 2. **Effect of Na²⁺ channel blockade, extracellular Ca²⁺ withdrawal, and L-type VGCC blockade on PACAP-induced [Ca²⁺]ᵢ elevation in BCCs.** *A*, exposure of Fura-2-loaded chromaffin cells to 100 nM PACAP, leading to a rapid Ca²⁺ rise followed by a sustained plateau phase (resting, 70 ± 2.09 nM; peak, 516 ± 55 nM; plateau, 272 ± 19 nM [Ca²⁺]ᵢ). *B*, lack of effect of 1 μM TTX on PACAP-evoked [Ca²⁺]ᵢ elevation (peak, 516 ± 55 nM [Ca²⁺]ᵢ). *C*, removal of extracellular Ca²⁺ abolishes the plateau phase but still results in an initial rise in [Ca²⁺]ᵢ that is, however, strongly reduced in amplitude in response to PACAP-38 (peak, 143 ± 19 nM [Ca²⁺]ᵢ). Effects of ICS depletion with thapsigargin and blockade of L-type VGCCs on PACAP-induced [Ca²⁺]ᵢ elevation (*D*), demonstrating that emptying of ICS and blocking of L-type VGCCs abolishes PACAP-evoked Ca²⁺ elevation in BCCs (resting, 58 ± 7 nM; Nimo, 73 ± 4.2 nM; Thap + Nimo, 211 ± 20 nM; PACAP + Nimo + Thap, 85 ± 5 nM [Ca²⁺]ᵢ). Plots represent the average ± S.E. of all cells (50–130 cells) recorded from three or four independent experiments. Calibrated [Ca²⁺]ᵢ values (nM) have been generated by converting 340/380-nm ratio values according to the method described by Grynckiewicz *et al.* (45).
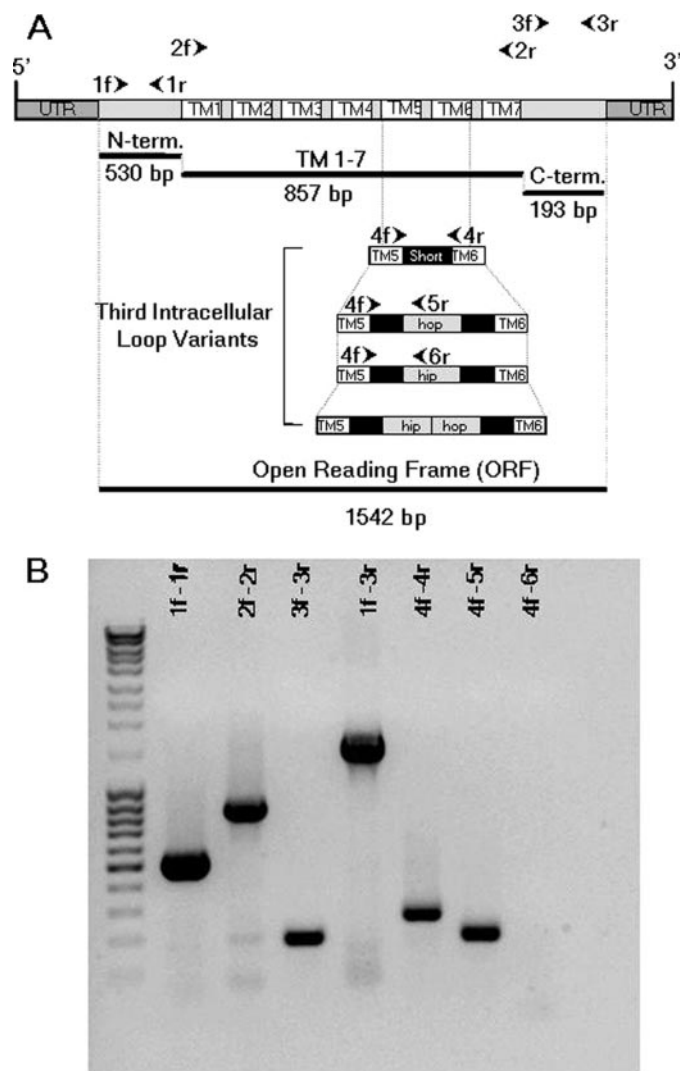

FIGURE 3. **Schematic representation of PCR-based identification and cloning of the BCC PAC1 receptor.** *A*, the previously published bovine brain PAC1 receptor sequence was used to design a series of primers that could amplify the receptor in three major overlapping segments that results in the generation of the entire open reading frame of the receptor. *B*, primer set 1 (*1f-1r*) was used to amplify the segment of the receptor from the start of the ORF to the beginning of transmembrane region 1. This resulted in the generation of a single 530-bp amplicon, indicating a full-length N terminus. Primer set B (*2f-2r*) was used to amplify TM regions 1–7, that includes both extracellular and intracellular loop regions of the receptor. An amplicon of 857 bp was generated, indicating a receptor variant with either a hop or hip cassette in the IC3 region. This was confirmed by the generation of a 271-bp amplicon using primer set 4 (*4f-4r*) designed to amplify the region between TM5 and TM6. To discriminate between the two cassettes, a reverse primer was designed to bind within either the hop (*5r*) or hip cassettes (*6r*). This resulted in the generation of a 200 bp using the hop specific primer (*4f-5r*), whereas no amplification was detected using the hip-specific primer (*4f-6r*), demonstrating that the bovine PAC1 receptor contains the hop cassette within the IC3 region. The C terminus region of the receptor from the TM7 to the end of the ORF was amplified using primer set C (*3f-3r*) and resulted in the generation of a 193-bp fragment. Sequence verification of the overlapping segments allowed the construction of a full-length sequence identical to the previously identified bovine brain PAC1ₕₒₚ receptor. The entire ORF was then amplified (*1f-3r*), and the full-length, 1542-bp cDNA was cloned into mammalian expression vector pcDNA3.

to AC, presumably through Gs, was reconstituted in these cells (Fig. 4*B*).

Exposure of NG108-15 cells stably expressing the bPAC1ₕₒₚ receptor to 100 nM PACAP resulted in a rapid rise in [Ca²⁺]ᵢ
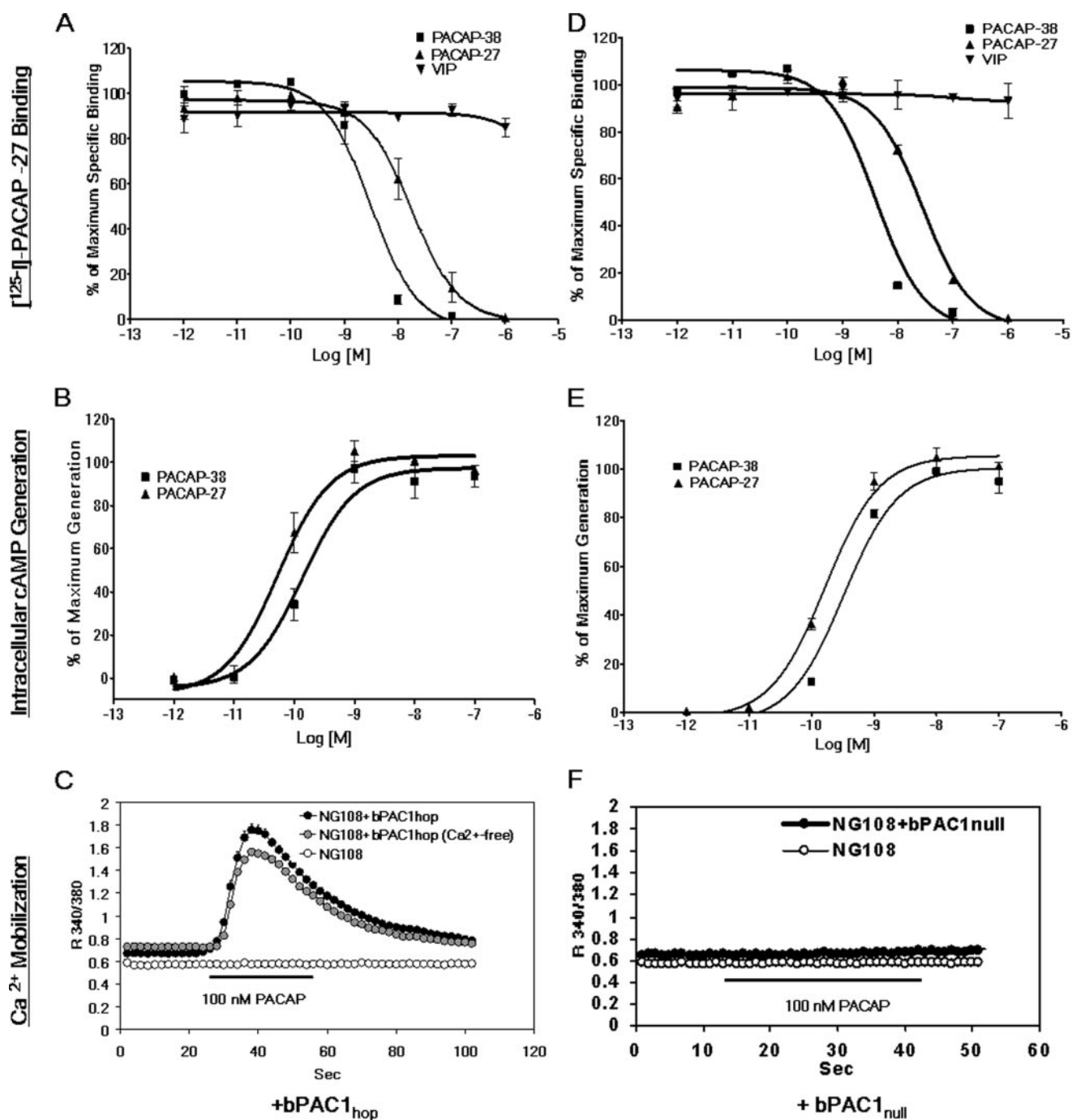
FIGURE 4. **Expression of the bPAC1$_{hop}$ and bPAC1$_{null}$ receptor in NG108-15 cells reconstitutes high affinity PACAP binding, activation of AC, and Ca^{2+} mobilization.** Competition of [^{125}I]PACAP-27 binding to bPAC1$_{hop}$-transfected (*A*) and bPAC1$_{null}$-transfected (*D*) NG108-15 cell membranes by unlabeled PACAP-38, PACAP-27, and VIP. Values are the mean ± S.E. of three or four independent experiments performed in duplicate. Binding is expressed as a percentage of maximum specific binding (*B/Bo* × 100) at each concentration of unlabeled peptide added. Dose-dependent increase in intracellular cAMP in NG108-15 cells stably expressing the bPAC1$_{hop}$ (*B*) and bPAC1$_{null}$ (*E*) receptor exposed to increasing concentrations of PACAP-38 or PACAP-27. Data shown are expressed as percentage of maximal intracellular cAMP stimulation. Values are expressed as the mean ± S.E. of triplicate determinations from two separate experiments. PACAP-triggered Ca^{2+} mobilization in NG108-15 cells expressing cloned bPAC1$_{hop}$, compared with naive NG108-15 cells in the presence (resting, 48 ± 1.9 nM; peak, 742.2 ± 61 nM; plateau, 53.5 ± 2.96 nM [Ca^{2+}]$_i$) or absence (resting, 61.9 ± 8.6 nM; resting Ca^{2+}-free KRB, 63.9 ± 4.1 nM; peak, 598.7 ± 58 nM; plateau, 68.6 + 2.3 nM [Ca^{2+}]$_i$) of extracellular Ca^{2+} (*C*). Exposure of bPAC1$_{null}$-expressing NG108-15 cells to PACAP did not stimulate Ca^{2+} elevation (56.3 ± 3.6 nM [Ca^{2+}]$_i$), similarly to naive NG108-15 cells (*F*). Values are the mean ± S.E. of 40–100 cells recorded from 3–6 independent experiments.

(resting, 48 ± 1.9 nM; peak, 742.2 ± 61 nM; plateau, 53.5 ± 2.96 nM [Ca^{2+}]$_i$) that was not observed in control untransfected NG108-15 cells (47 ± 1.09 nM [Ca^{2+}]$_i$), confirming this as a bPAC1$_{hop}$ receptor-mediated event (Fig. 4*C*). Removal of extracellular Ca^{2+} did not affect the rapid initial rise of [Ca^{2+}]$_i$ fol-

lowing PACAP (resting, 61.9 ± 8.6 nM; resting Ca^{2+}-free KRB, 63.9 ± 4.1 nM; peak, 598.7 ± 58 nM; plateau, 68.6 ± 2.3 nM [Ca^{2+}]$_i$), indicating that the bulk of the Ca^{2+} release into the cytoplasm was contributed by intracellular stores (Fig. 4*C*) with no obvious Ca^{2+} influx "plateau phase" as observed in the

TABLE 1

Ligand binding properties of bPAC1$_{hop}$- and bPAC1$_{null}$-expressing NG108-15 and PC12-G cells

Receptor binding affinity (K_d) and receptor density (B_{max}) were determined through homologous competition binding experiments as described in Ref. 70.

Cell type	Receptor	PACAP-38 K_d	PACAP-27 K_d	PACAP-38 B_{max}
		nM	*nM*	*pM/mg*
NG108-15	bPAC1$_{hop}$	4	18	11
	bPAC1$_{null}$	4	28	12
PC12-G	bPAC1$_{hop}$	4	27	11
	bPAC1$_{null}$	8	38	21

BCCs. $[Ca^{2+}]_i$ elevation stimulated through bPAC1$_{hop}$ in NG108-15 cells was completely blocked by pretreatment with the phospholipase C inhibitor U73122 (10 μM; data not shown), consistent with mediation of $[Ca^{2+}]_i$ elevation through IP$_3$.

Removal of the Hop Domain from the IC3 Region of Bovine PAC1 Receptor Abolishes Receptor Coupling to $[Ca^{2+}]_i$ Mobilization from ICS without Affecting the Generation of Intracellular cAMP in NG108-15 Cells—Similarly to bPAC1$_{hop}$, cell membranes from bPAC1$_{null}$-expressing NG108-15 cells displayed high affinity [^{125}I]PACAP-27 binding that could be specifically competed for by unlabeled PACAP-38 and PACAP-27 with IC$_{50}$ values of 4 and 30 nM, respectively, and was not displaced by VIP (Fig. 4*D*). Exposure to PACAP-38 and PACAP-27 also stimulated intracellular cAMP generation in a concentration-dependent manner with IC$_{50}$ values of 0.3 and 0.17 nM, respectively (Fig. 4*E*). These results demonstrated that removal of the hop cassette from the IC3 region of bPAC1 did not impair the N terminus binding properties of the receptor, receptor trafficking to the plasma membrane compartment, or its ability to couple to AC through G$_s$ in NG108-15 cells. Both bPAC1$_{hop}$- and bPAC1$_{null}$-expressing NG108-15 cells had identical receptor levels ($B_{max} = 11$–12 pM receptor/mg of protein) (see Table 1), determined using data generated from homologous competitive binding experiments (Fig. 4, *A* and *D*).

Expression of the bPAC1$_{null}$ receptor in NG108-15 cells at a density equivalent to that of bPAC1$_{hop}$ reconstituted both high affinity PACAP-27 binding and PACAP-dependent cAMP generation. However, PACAP did not evoke $[Ca^{2+}]_i$ elevation in bPAC1$_{null}$-expressing NG108-15 cells (56.3 ± 3.6 nM $[Ca^{2+}]_i$) (Fig. 4*F*), suggesting that the hop cassette plays a critical role in transducing PACAP-dependent Ca^{2+} mobilization signaling in neural cells.

Expression of bPAC1 Confers High Density PACAP Binding and Hop-dependent Coupling to Ca^{2+} Mobilization from ICS and Ca^{2+} Influx in PC12-G Cells—Our observations in NG108-15 cells (above) suggested that, unlike results predicted from regulation of PLC coupling through both PAC1$_{hop}$ and PAC1$_{null}$ receptors reported in nonneuronal cells, regulation of Ca^{2+} mobilization by PAC1 receptor stimulation in neural cell lines may be specific to the hop variant of the receptor. We wanted to confirm these results in another neural cell line and extend them to analysis of functional sequelae of Ca^{2+} mobilization by PACAP leading to exocytosis. bPAC1$_{hop}$ and bPAC1$_{null}$ variants were therefore expressed in rat PC12-G cells, a well characterized neuroendocrine cell line in which Ca^{2+}-dependent catecholamine secretion has been well studied.

Expression of the bPAC1$_{hop}$ or bPAC1$_{null}$ receptors in PC12-G cells reconstituted high density and high affinity [^{125}I]PACAP-27 binding that could be specifically competed for by unlabeled PACAP-38 and PACAP-27 with IC$_{50}$ values of 4.8 and 26 nM, respectively, for bPAC1$_{hop}$ (Fig. 5*A*) and 7.5 and 38 nM, respectively, for bPAC1$_{null}$ (Fig. 5*B*). VIP did not compete for [^{125}I]PACAP-27 binding to either the endogenous rat or either of the bovine receptors. Mock-transfected PC12-G cells expressed high affinity but very low density [^{125}I]PACAP-27 binding (<10% of total specific binding measured in PC12-G cells transfected with bPAC1$_{hop}$; data not shown). Treatment of either naive, bPAC1$_{hop}$-transfected, or bPAC1$_{null}$-transfected PC12-G cells with varying concentrations of PACAP-38 resulted in a potent concentration-dependent elevation of intracellular cAMP levels at comparable levels with EC$_{50}$ values of 0.78 nM (PC12-G), 1.2 nM (bPAC1$_{hop}$), and 3 nM (bPAC1$_{null}$) (Fig. 5, *B* and *D*). These data indicate that PC12-G cells are capable of appropriate trafficking, expression, and G-protein coupling of PAC1 receptors. The endogenous PAC1 receptor appeared to be maximally efficiently coupled to AC through Gα_s in PC12-G cells, since cAMP production induced by 100 nM PACAP-38 in PC12-G cells was not further increased by the >10-fold increase in PACAP-27 binding after expression of bPAC1$_{hop}$ or bPAC1$_{null}$ and is equivalent to that generated by direct supramaximal stimulation of adenylate cyclase with 25 μM forskolin (results not shown).

Ca^{2+} signaling was next examined in bPAC1$_{hop}$-expressing, bPAC1$_{null}$-expressing, or naive PC12-G cells following transient transfection. A GFP expression vector served as a marker of transfection efficiency to discriminate between bPAC1- and non-bPAC1-expressing PC12-G cells for single cell Ca^{2+} imaging (Fig. 6). Following Fura-2 loading, GFP-positive and -negative cells were identified (Fig. 6, *inset A*). Expression of GFP alone affected neither basal $[Ca^{2+}]_i$ nor elevation of $[Ca^{2+}]_i$ elicited by either 100 nM PACAP or 40 mM KCl (data not shown). bPAC1$_{hop}$-expressing (GFP-positive) cells responded to exposure to 100 nM PACAP with a large and rapid rise in $[Ca^{2+}]_i$ typical of Ca^{2+} release from ICS (resting, 64.6 ± 3.95 nM; peak, 731 ± 58 nM; plateau, 213 ± 26 nM $[Ca^{2+}]_i$). This phase was followed by a prolonged phase of $[Ca^{2+}]_i$ elevation, attributable to extracellular Ca^{2+} influx (Fig. 6), as shown previously in BCCs (Fig. 2*A*; see Ref. 8). Untransfected cells responded to PACAP treatment with very small increases in $[Ca^{2+}]_i$ that reflect the limited coupling of endogenous PAC1 receptors expressed in PC12-G cells with Ca^{2+} mobilization and influx (Fig. 6) (resting, 65.3 ± 3.8 nM; peak, 175 ± 16 nM; plateau, 153 ± 11.3 nM $[Ca^{2+}]_i$).

We next investigated whether reconstitution of $[Ca^{2+}]_i$ elevation by bPAC1 was specifically dependent on the presence of the hop cassette in PC12-G cells, as observed in NG108-15 cells. Expression of bPAC1$_{null}$ in PC12-G cells, with GFP as a marker for transfection, allowed Fura-2 visualization of $[Ca^{2+}]_i$ following exposure to PACAP-38, which was not elevated beyond the small rise observed in untransfected PC12-G cells (Fig. 6). Thus, removal of the hop cassette uncoupled the PAC1 receptor from its ability to promote Ca^{2+} mobilization from ICS as well as Ca^{2+} influx, implicating the hop cassette within IC3 as a critical determinant in PAC1 receptor coupling to both Ca^{2+} mobili-
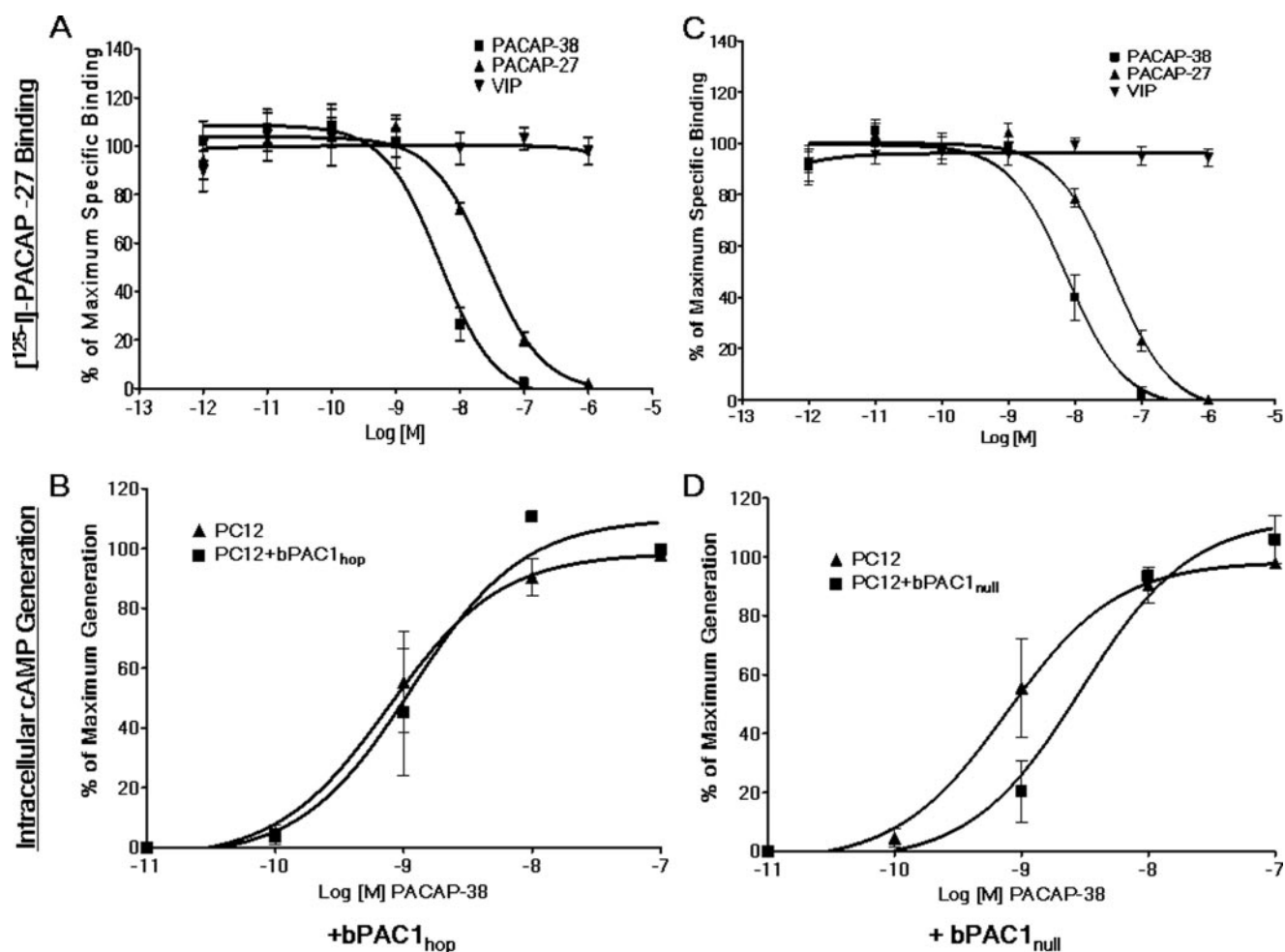
FIGURE 5. **Expression of the bPAC1$_{hop}$ and bPAC1$_{null}$ receptor in PC12-G cells confers high affinity PACAP binding and cAMP generation.** Shown is competition of [^{125}I]PACAP-27 binding to bPAC1$_{hop}$-transfected (*A*) and bPAC1$_{null}$-transfected (*C*) PC12-G cell membranes by unlabeled PACAP-38, PACAP-27, and VIP. Mock-transfected PC12-G cells displayed less than 10% of the total specific binding observed for bPAC1$_{hop}$-transfected cells (results not shown). Values are the mean ± S.E. of four independent experiments performed in duplicate. Binding is expressed as a percentage of maximum specific binding (*B/Bo* × 100) at each concentration of unlabeled peptide added. Generation of intracellular cAMP following exposure of naive and bPAC1$_{hop}$-expressing (*B*) and bPAC1$_{null}$-expressing (*D*) PC12-G cells to PACAP-38 and PACAP-27. Data are expressed as a percentage of maximal intracellular cAMP stimulation and as the mean ± S.E. of experiments performed in triplicate two or three times.

zation from ICS and Ca²⁺ influx (resting, 65.8 ± 3.4 nM; peak, 115 ± 8.7 nM; plateau, 90 ± 4.6 nM [Ca²⁺]$_i$).

PACAP stimulation of bPAC1$_{hop}$-expressing PC12-G cells in Ca²⁺-free medium prevented the plateau phase of [Ca²⁺]$_i$ elevation, indicating its dependence on extracellular Ca²⁺ influx following Ca²⁺ mobilization (Fig. 7). These findings indicate that PC12-G cells express molecular components required for PAC1$_{hop}$ coupling to [Ca²⁺]$_i$ elevation through Ca²⁺ mobilization from ICS and via extracellular Ca²⁺ entry, provided that the receptor is expressed at sufficient density (Ca²⁺-free KRB: resting, 70.23 ± 4.9 nM; peak, 259.33 ± 21 nM; plateau, 67.27 ± 12.17 nM; Ca²⁺-KRB: resting, 62.3 ± 2.5 nM; peak, 424.31 ± 23.6 nM; plateau, 233.1 ± 4 nM [Ca²⁺]$_i$). These results are further confirmed by expression of the rat PAC1$_{hop}$ receptor under the control of the cytomegalovirus promoter, which increased rPAC1$_{hop}$ expression in PC12-G cells around 10-fold and also reconstituted both PACAP-mediated Ca²⁺ mobilization from ICS (Ca²⁺ peak) and influx (Ca²⁺ plateau) in PC12-G cells (data not shown).

Expression of bPAC1$_{hop}$ Confers PACAP-evoked [³H]Norepinephrine Release in PC12-G Cells—PC12-G cells express very low levels of PAC1 and do not exhibit either Ca²⁺ mobilization or a substantial Ca²⁺ influx following exposure to PACAP in KRB (Fig. 6). We hypothesized that these cells might lack competence for PACAP-evoked secretion, unlike some PC12 cell lines that are competent for both PACAP-evoked Ca²⁺ influx and catecholamine secretion (28), and would therefore represent an effective model for reconstitution of PAC1-dependent catecholamine secretion.

As demonstrated in Fig. 8*A*, PC12-G cells efficiently accumulate [³H]norepinephrine yet fail to release it in response to PACAP-evoked secretion in KRB, suggesting that the low density of endogenously expressed PAC1 receptors in PC12-G cells do not generate a sufficient Ca²⁺ signal for regulated exocytosis. Membrane depolarization of naive PC12-G with 55 mM KCl caused significant secretion of norepinephrine (30% of total content) (Fig. 8*A*), thus confirming sufficient uptake/loading of cells with [³H]norepinephrine. In contrast, bPAC1$_{hop}$-express-
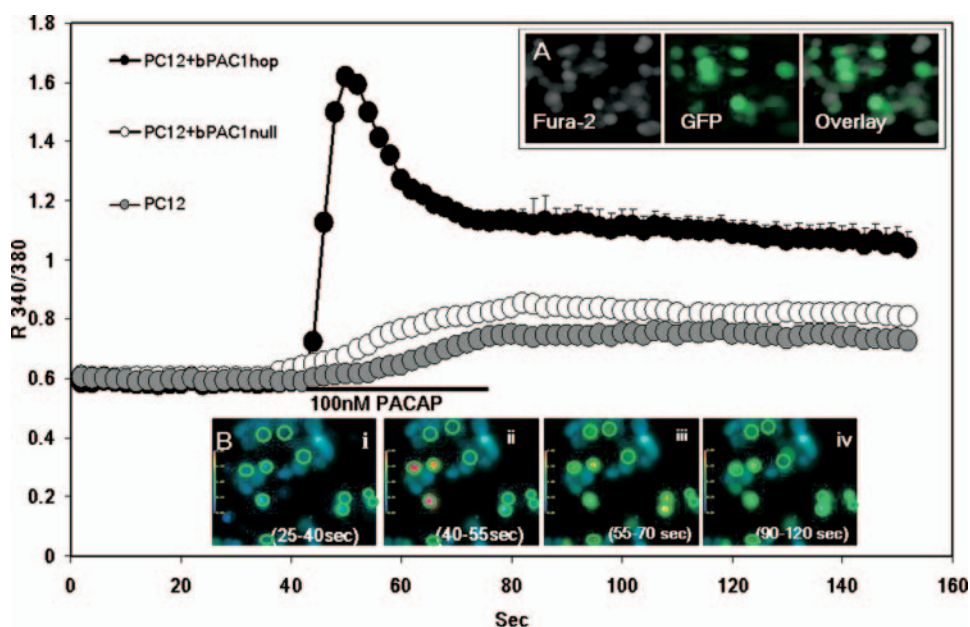
FIGURE 6. **Expression of the bPAC1$_{hop}$ receptor reconstitutes intracellular Ca²⁺ mobilization and influx in PC12-G cells that can be abolished by removing the hop domain of the bovine PAC1 receptor.** PC12-G cells were transiently transfected with bPAC1$_{hop}$ or bPAC1$_{null}$ expression vectors and a GFP expression marker vector and loaded with Fura-2. Cells were preidentified as untransfected or transfected based on GFP fluorescence (*inset A*) and monitored for changes in [Ca²⁺]$_i$ measured as the 510-nm emission ratio after excitation at 340 and 380 nm. Exposure of bPAC1$_{hop}$ (GFP-positive) cells to 100 nM PACAP resulted in a rapid rise in Ca²⁺ that was followed by a persisting plateau phase (resting, 64.6 ± 3.95 nM; spike, 731 ± 58 nM; plateau, 213 ± 26 nM [Ca²⁺]$_i$) (*black circle*) that was not observed in naive untransfected (GFP-negative) PC12-G cells (*gray circle*) (resting, 65.3 ± 3.8 nM; after PACAP exposure, 175 ± 16 nM; plateau, 53 ± 11.3 nM [Ca²⁺]$_i$). As demonstrated in *inset B*, only cells expressing GFP (*circled*) exclusively responded to PACAP. GFP-positive PC12-G cells expressing the bPAC1$_{null}$ receptor, created by removing the hop domain, stimulated with 100 nM PACAP failed to mediate both Ca²⁺ mobilization or influx (*open circle*) in PC12-G cells (resting, 65.8 ± 3.4 nM; PACAP exposure, 115 ± 8.7 nM; plateau, 90 ± 4.6 nM [Ca²⁺]$_i$). All images were taken using a 40× objective with oil immersion. *Plots* represent the average ± S.E. of 40–100 cells recorded from three or four independent experiments. Calibrated [Ca²⁺]$_i$ values (nM) were generated by converting 340/380-nm ratio values according to the method described by Grynckiewicz *et al.* (45).

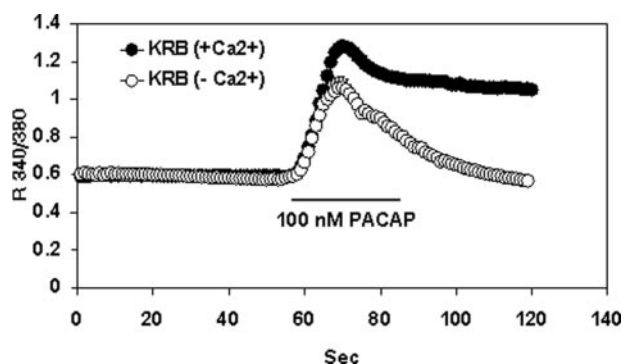FIGURE 7. **PACAP-evoked Ca²⁺ elevation in bPAC1$_{hop}$-expressing PC12-G consists of both Ca²⁺ mobilization from ICS and extracellular Ca²⁺ influx.** Treatment of Fura-2-loaded PC12-G cells stably expressing the bPAC1$_{hop}$ receptor with 100 nM PACAP in the presence (*filled circle*) or absence (*open circle*) of extracellular Ca²⁺ indicates that PACAP-evoked Ca²⁺ elevation consists of two events: intracellular Ca²⁺ mobilization from intracellular stores (base line, 62.3 ± 2.5 nM; peak, 424.31 ± 23.6 nM [Ca²⁺]$_i$) and extracellular influx (plateau, 233 ± 4 nM [Ca²⁺]$_i$) as indicated by the presence of the initial Ca²⁺ spike (resting, 70.23 ± 4.9 nM; peak, 259.33 ± 21 nM [Ca²⁺]$_i$) and absence of the persistent plateau phase (67.27 ± 12.17 nM [Ca²⁺]$_i$) in experiments carried out in Ca²⁺-free KRB buffer. All images were acquired using a ×40 oil immersion lens. Plots represent the average ± S.E. of 60–120 cells recorded from three or four independent experiments. Calibrated [Ca²⁺]$_i$ values (nM) have been generated by converting 340/380-nm ratio values according to the method described by Grynckiewicz *et al.* (45).

ing PC12-G cells exhibit robust stimulation of catecholamine release in response to 30-min exposure to 100 nM PACAP (30% of total content) (Fig. 8*B*), which is abolished upon removal of

Ca²⁺ from the medium (Fig. 8*C*), demonstrating that expression of the bPAC1$_{hop}$ receptor in PC12-G cells confers Ca²⁺ influx-dependent secretion evoked by PACAP, as previously demonstrated in BCCs.

DISCUSSION

The structural basis for PAC1 receptor coupling to Ca²⁺ mobilization and influx has not been previously addressed in a heterologous neuroendocrine cell culture system; nor has the structural basis for PAC1-dependent Ca²⁺ mobilization from ICS been investigated, which along with elevation of intracellular cAMP, is the hallmark of combinatorial signaling by the slow transmitter PACAP. The bPAC1$_{hop}$ receptor isolated from BCCs contains an intact full-length N terminus and a hop cassette in IC3 as previously identified in rat and human tissues and bovine brain. This receptor variant binds PACAP with high affinity and activates second messenger systems, such as AC and presumably PLC. This phenotype is common to most of the known PAC1 receptor splice variants, which have been examined upon expression in nonneuroendocrine heterologous cell lines (22, 50). Expression of the PAC1$_{hop}$ variant is sufficient for coupling PAC1 receptor occupancy to Ca²⁺ signaling, leading to exocytosis. The ability to couple to Ca²⁺ influx has been previously ascribed to a transmembrane domain 4 variant of PAC1 (26), but this variant has never been demonstrated to cause Ca²⁺ influx in a neuroendocrine cell, and the possibility of its natural occurrence has been challenged on structural and genetic grounds (14). In contrast, transfer of the bPAC1$_{hop}$ receptor to PC12-G cells simultaneously conferred PACAP-dependent Ca²⁺ coupling and catecholamine secretion. The ability of PACAP to cause large and long lasting changes in [Ca²⁺]$_i$, required to trigger regulated exocytosis, provides a mechanism for the physiological role of PACAP as a slow transmitter subserving long lasting adrenal catecholamine secretion in response to metabolic and other stressors (9). We have further shown that transfer of PACAP-dependent secretory competence is specific for PAC1 receptor expression at levels found at or near physiological receptor density (*i.e.* that found in bovine chromaffin cells) and that Ca²⁺ coupling, but not coupling to AC, is highly specific for the hop cassette in IC3 of the receptor.

The hop and null forms of the PAC1 receptor are the major variants found in rats and humans, whereas systematic comparison of variants present in bovine tissues has not been carried out except in the adrenal medulla (*i.e.* this study). With respect to studies in heterologous cells, no dif-
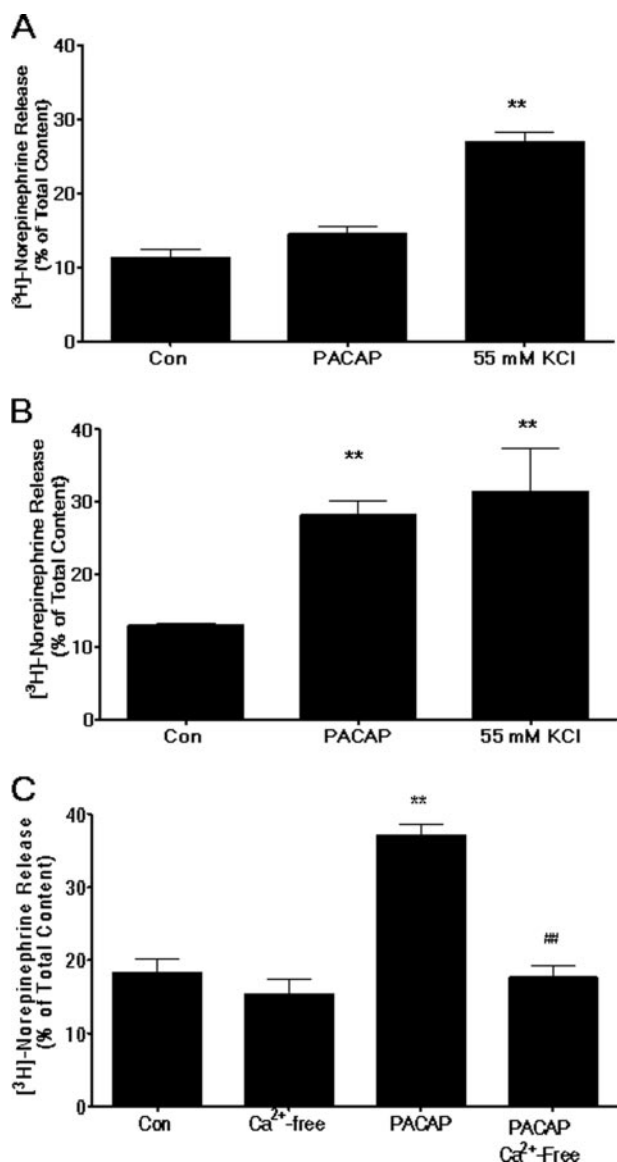
FIGURE 8. **Expression of the bPAC1$_{hop}$ receptor in PC12-G cells reconstitutes PACAP-evoked Ca^{2+} influx-dependent catecholamine secretion.** Naive PC12-G cells loaded with [^{3}H]norepinephrine were stimulated with 100 nM PACAP or 55 mM KCl. In comparison with KCl-evoked norepinephrine secretion through membrane depolarization and opening of VGCCs, PACAP did not stimulate the secretion of norepinephrine in naive PC12-G cells (*A*). Transfection of PC12-G cells with the bPAC1$_{hop}$ receptor reconstituted PACAP-evoked norepinephrine secretion that was significantly higher compared with naive PC12-G cells (*B*). Removal of extracellular Ca^{2+} abolished PACAP-evoked norepinephrine secretion without affecting basal secretion (*C*). Values represent the mean $\pm$ S.E. of triplicate wells obtained from 3–7 independent experiments. Differences between control and treatment groups were determined using one-way analysis of variance followed by *post hoc* Tukey's multiple comparison test. **, $p < 0.001$ compared with corresponding control; ##, $p < 0.001$ compared with corresponding treatment.

ferences between these two major variants have been demonstrated that could account for their differential involvement in neurosecretion. Thus, the human and rat hop and null receptors have both been shown to be efficacious in coupling PAC1 receptor occupancy to PLC-mediated IP$_3$ generation, presumably through G$_q$, in nonneuroendocrine cell lines (22–25). Our current findings, however, demonstrate that in neural cell lines, such as NG108-15 and PC12-G, loss of the hop cassette results in a PAC1 receptor

that is clearly deficient in coupling to Ca^{2+} mobilization and influx, although it is fully competent for PACAP-dependent coupling to activation of AC.

PC12 cells are a commonly employed cellular model for investigating the neurotrophic effects of PACAP (51). Unlike some other PC12 cell variants, binding studies demonstrated that the PC12-G cells used here expressed very low levels of PAC1 receptors ($\sim$10 times less, as measured by [^{125}I]PACAP-27 binding, than in bPAC1$_{hop}$-transfected PC12-G cells and severalfold less than in BCCs) and displayed only small elevations in [Ca^{2+}]$_i$ following exposure to PACAP. Previous studies have demonstrated the ability of PACAP to induce relatively large Ca^{2+} transients in some PC12 cell lines, perhaps due to higher levels of expression of PAC1$_{hop}$ than in PC12-G (52–54) and similar commonly employed PC12 cell lines (55). Reverse transcription-PCR analysis of the naive PC12-G cells used in our studies revealed the presence of two PAC1 receptor variants, PAC1$_{hop}$ and PAC1$_{hip}$, which are expressed at similar but very low levels (56).[4] We found that increasing the expression of the endogenous rat PAC1$_{hop}$ receptor to levels similar to those of bPAC1$_{hop}$ in BCCs or in bPAC1$_{hop}$-PC12-G cells also reconstituted coupling to both intracellular Ca^{2+} mobilization and Ca^{2+} influx. Endogenous PAC1 expression in neurons *in vivo* can vary significantly in response to physiological and pathophysiological stimuli (55, 57). The ability of PAC1$_{hop}$ to couple to Ca^{2+} mobilization and influx in combination with cAMP, rather than to cAMP alone, upon up-regulation of receptor expression *in vivo*, may correspondingly alter the postsynaptic slow neurotransmitter properties of PACAP, uncovering a new type of GPCR functional regulation through expression level-dependent coupling to cAMP alone (at low receptor density) or cAMP and Ca^{2+} mobilization and influx (at higher receptor density).

One mechanism suggested for PACAP action on secretion through PAC1 receptors in various cell types is via cAMP/protein kinase A-mediated protein phosphorylation (31, 32, 53, 58), possibly of VGCCs themselves, with a resultant potentiation of ion channel opening probability and duration (59–63). However, as reported here, cAMP elevation alone following exposure to forskolin failed to mimic PACAP-evoked secretion or Ca^{2+} elevation in BCCs or PC12-G cells, suggesting that bPAC1$_{hop}$-mediated cAMP generation alone is insufficient for initiating PACAP-stimulated Ca^{2+} elevation, influx, or acute secretion. However, a modulatory role of cAMP in conjunction with [Ca^{2+}]$_i$ to maintain long term PACAP-evoked secretion from chromaffin cells is plausible and likely, based on partial inhibition of PACAP-stimulated secretion from perfused adrenal medulla by inhibition of protein kinase A (30).

Two major hypotheses have been proposed for initiation of [Ca^{2+}]$_i$ elevation by PACAP and other GPCR ligands in excitable (neuroendocrine) cells. The first is that receptor occupancy mediates membrane depolarization and subsequent facilitation of VGCC opening. PACAP has been variously shown to influence membrane potentials in supraoptic neurons (64), pinealocytes (34), sympathetic neurons (17), suprachiasmatic nuclear neurons (65), and chromaffin cells (36), through

---

[4] T. Mustafa, unpublished results.

mechanisms proposed to involve Na$^+$ influx through Na$^+$ channels, Na$^+$ or Ca^{2+} entry through nonselective cation channels, or inhibition of outwardly directed K$^+$ channels leading to depolarization sufficient to voltage-gate the opening of VGCCs (17, 34–36, 62, 63). The second hypothesis is that PACAP affects Ca^{2+} entry via prior activation of PLC-mediated Ca^{2+} release from IP$_3$-sensitive ICS (17), perhaps also requiring co-activation of protein kinase C (65), with PACAP-mediated Ca^{2+} influx dependent on PLC-IP$_3$-mediated Ca^{2+} mobilization from ICS. This mechanism is the one most strongly supported by our results with bPAC1$_{hop}$, due to the association of the hop cassette with Ca^{2+} mobilization in NG108-15 cells and with both mobilization and influx of Ca^{2+} in PC12-G cells. Our identification of the specific PAC1 variant and the relevant IC3 domain, which supports PACAP-mediated Ca^{2+} mobilization and influx in chromaffin cells, provides an important mechanistic insight into PAC1-Ca^{2+} coupling and an experimental avenue for further exploration of the steps underlying initiation of Ca^{2+} influx via this important class II GPCR.

We have provided evidence that removal of the hop cassette from the IC3 region of the bPAC1 receptor eliminates its ability to mediate PACAP-evoked Ca^{2+} mobilization from ICS in both PC12-G and NG108-15 cells despite retention of high affinity binding and cAMP generation by PACAP. The requirement for a discrete region of the IC3 loop of the PAC1 receptor to activate Ca^{2+} mobilization, Ca^{2+} influx, and exocytotic secretion suggests the possibility that several components required for regulated exocytosis may be brought into close proximity through the hop-dependent formation of a specific signaling complex to trigger PACAP-dependent neurosecretion. Ronaldson and co-workers (25) have demonstrated that the small GTP-binding protein ARF6 (ADP-ribosylation factor-6) specifically interacts with the hop cassette to activate phospholipase D (24, 25), and the role of ARF6 in membrane trafficking, synaptic vesicle biogenesis (66), and Ca^{2+}-dependent large dense core vesicle exocytosis in both PC12 and chromaffin cells has been well established (67, 68). ARF6 or a related GTPase may have a role in PAC1$_{hop}$-mediated exocytosis through formation of such a complex.

In conclusion, we have demonstrated that a single PAC1 receptor variant, bPAC1$_{hop}$, exists in BCCs and couples PAC1 receptor occupancy by PACAP to Ca^{2+} mobilization, influx, and neurotransmitter release from large dense core vesicles. This mode of signaling appears to be neuroendocrine cell-specific and probably depends on the presence of specific signaling molecules in neuroendocrine cells. The demonstration that Ca^{2+} coupling for secretion absolutely requires the hop cassette should allow rapid elucidation of the molecular bases for the sequential processes of Ca^{2+} mobilization and influx preceding exocytosis evoked by PACAP through the class II G-protein-coupled receptor, PAC1.

REFERENCES

1. O'Farrell, M., and Marley, P. D. (1997) *Naunyn-Schmiedeberg's Arch. Pharmacol.* **356,** 536–542
2. Hahm, S. H., Hsu, C.-M., and Eiden, L. E. (1998) *J. Mol. Neurosci.* **11,** 1–15
3. Watanabe, T., Masuo, Y., Matsumoto, H., Suzuki, N., Ohtaki, T., Masuda, Y., Kitada, C., Tsuda, M., and Fujino, M. (1992) *Biochem. Biophys. Res. Commun.* **182,** 403–411
4. Isobe, K., Hakai, T., and Takuwa, Y. (1993) *Endocrinology* **132,** 1757–1765
5. Geng, G., Gaspo, R., Trabelsi, F., and Yamaguchi, N. (1997) *Am. J. Physiol.* **273,** R1339–R1345
6. Lamouche, S., Martineau, D., and Yamaguchi, N. (1999) *Am. J. Physiol.* **276,** R162–R170
7. Mazzocchi, G., Malendowicz, L. K., Rebuffat, P., Gottardo, L., and Nussdorfer, G. G. (2002) *J. Clin. Endocrinol. Metab.* **87,** 2575–2580
8. Hamelink, C., Lee, H.-W., Grimaldi, M., and Eiden, L. E. (2002) *J. Neurosci.* **22,** 5310–5320
9. Hamelink, C., Tjurmina, O., Damadzic, R., Young, W. S., Weihe, E., Lee, H.-W., and Eiden, L. E. (2002) *Proc. Natl. Acad. Sci. U. S. A.* **99,** 461–466
10. Marley, P. D., Cheung, C. Y., Thomson, K. A., and Murphy, R. (1996) *J. Autonom. Nerv. Syst.* **60,** 141–146
11. Babinski, K., Bodart, V., Roy, M., De Léan, A., and Ong, H. (1996) *Neuropeptides* **30,** 572–582
12. Lee, H.-W., Hahm, S. H., Hsu, C.-M., and Eiden, L. E. (1999) *J. Neurochem.* **73,** 1769–1772
13. Hamelink, C., Weihe, E., and Eiden, L. E. (2003) in *Pituitary Adenylate Cyclase-activating Polypeptide* (Vaudry, H., and Arimura, A., eds) pp. 227–249, Kluwer-Academic Press, New York
14. Mustafa, T., and Eiden, L. E. (2006) in *Handbook of Neurochemistry and Molecular Neurobiology: Neuroactive Peptides and Proteins* (Lim, R., ed) pp. 463–498, Springer, Heidelberg
15. Sabban, E. L., Hiremagalur, B., Nankova, B., and Kvetnansky, R. (1995) *Ann. N. Y. Acad. Sci.* **771,** 327–338
16. Beaudet, M. M., Braas, K. M., and May, V. (1998) *J. Neurobiol.* **36,** 325–336
17. Beaudet, M. M., Parsons, R. L., Braas, K. M., and May, V. (2000) *J. Neurosci.* **20,** 7353–7361
18. Braas, K. M., and May, V. (1996) *Ann. N. Y. Acad. Sci.* **805,** 204–216
19. Braas, K. M., and May, V. (1999) *J. Biol. Chem.* **274,** 27702–27710
20. Pantaloni, C., Brabet, P., Bilanges, B., Dumuis, A., Houssami, S., Spengler, D., Bockaert, J., and Journot, L. (1996) *J. Biol. Chem.* **271,** 22146–22151
21. Dautzenberg, F. M., Mevenkamp, G., Wille, S., and Hauger, R. L. (1999) *J. Neuroendocrinol.* **11,** 941–949
22. Spengler, D., Bweber, C., Pantaloni, C., Hlsboer, F., Bockaert, J., Seeburg, P. H., and Journot, L. (1993) *Nature* **365,** 170–175
23. Pisegna, J. R., and Wank, S. A. (1996) *J. Biol. Chem.* **271,** 17267–17274
24. McCulloch, D. A., Lutz, E. M., Johnson, M. S., Robertson, D. N., MacKenzie, C. J., Holland, P. J., and Mitchell, R. (2001) *Mol. Pharmacol.* **59,** 1523–1532
25. Ronaldson, E., Robertson, D. N., Johnson, M. S., Holland, P. J., Mitchell, R., and Lutz, E. M. (2002) *Regul. Pept.* **109,** 193–198
26. Chatterjee, T. K., Sharma, R. V., and Fisher, R. A. (1996) *J. Biol. Chem.* **271,** 32226–32232
27. Eiden, L. E. (2003) Signaling during Exocytosis in *Handbook of Cell Signaling* (Bradshaw, R., and Dennis, E., eds) pp. 375–392, Academic Press, Inc., New York
28. Taupenot, L., Mahata, M., Mahata, S. K., and O'Connor, D. T. (1999) *Hypertension* **34,** 1152–1162
29. Fukushima, Y., Nagayama, T., kawashima, H., Hikichi, H., Yoshida, M., Suzuki-Kusaba, M., Hisa, H., Kimura, T., and Satoh, S. (2001) *Am. J. Physiol.* **281,** R495–R501
30. Przywara, D. A., Xi, G., Angelilli, L., Wakade, T. D., and Wakade, A. R. (1996) *J. Biol. Chem.* **271,** 10545–10550
31. Tanaka, K., Shibuya, I., Harayama, N., Nomura, M., Kabashima, N., Ueta, Y., and Yamashita, H. (1997) *Endocrinology* **138,** 4086–4095
32. Shioda, S., Yada, T., Muroya, S., Uramura, S., Nakajo, S., Ohtaki, H., Hori, T., Shimoda, Y., and Funahashi, H. (2000) *Ann. N. Y. Acad. Sci.* **921,** 211–217
33. Turquier, V., Yon, L., Grumolato, L., Alexandre, D., Fournier, A., Vaudry, H., and Anouar, Y. (2001) *Mol. Pharmacol.* **60,** 42–52

34. Darvish, N., and Russell, J. T. (1998) *J. Neurophysiol.* **79,** 2546–2556
35. May, V., Beaudet, M. M., Parsons, R. L., Hardwick, J. C., Gauthier, E. A., Durda, J. P., and Braas, K. M. (1998) *Ann. N. Y. Acad. Sci.* **865,** 164–175
36. Tanaka, K., Shibuya, I., Nagamoto, T., Yamasha, H., and Kanno, T. (1996) *Endocrinology* **137,** 956–966
37. Eiden, L. E., Giraud, P., Affolter, H.-U., Herbert, E., and Hotchkiss, A. J. (1984) *Proc. Natl. Acad. Sci. U. S. A.* **81,** 3949–3953
38. Fenwick, E. M., Fajdiga, P. B., Howe, N. B. S., and Livett, B. G. (1978) *J. Cell Biol.* **76,** 12–30
39. Miyamoto, Y., Habata, Y., Ohtaki, T., Masuda, Y., Ogi, K., Onda, H., and Fujino, M. (1994) *Biochim. Biophys. Acta* **1218,** 297–307
40. Horton, R. M., Cai, Z. L., Ho, S. N., and Pease, L. R. (1990) *BioTechniques* **8,** 528–535
41. Lee, J., Lee, H. J., Shin, M. K., and Ryu, W. S. (2004) *BioTechniques* **36,** 398–400
42. Rausch, D. M., Iacangelo, A. L., and Eiden, L. E. (1988) *Mol. Endocrinol.* **2,** 921–927
43. Mustafa, T., Chai, S. Y., Mendelsohn, F. A., Moeller, I., and Albiston, A. L. (2001) *J. Neurochem.* **76,** 1679–1687
44. Grimaldi, M., Maratos, M., and Verma, A. (2003) *J. Neurosci.* **23,** 4737–4745
45. Grynkiewicz, G., Poenie, M., and Tsien, R. Y. (1985) *J. Biol. Chem.* **260,** 3440–3450
46. Eiden, L. E., Iacangelo, A., Hsu, C.-M., Hotchkiss, A. J., Bader, M.-F., and Aunis, D. (1987) *J. Neurochem.* **49,** 65–74
47. Daniel, P. B., Kieffer, T. J., Leech, C. A., and Habener, J. F. (2001) *J. Biol. Chem.* **276,** 12938–12944
48. Pisegna, J. R., and Wank, S. A. (1993) *Proc. Natl. Acad. Sci. U. S. A.* **90,** 6345–6349
49. Hamprecht, B., Glaser, T., Reiser, G., Bayer, E., and Propst, F. (1985) *Methods Enzymol.* **109,** 316–341
50. Pisegna, J. R., Moody, T. W., and Wank, S. A. (1996) *Ann. N. Y. Acad. Sci.* **805,** 54–64
51. Vaudry, D., Stork, P. J., Lazarovici, P., and Eiden, L. E. (2002) *Science* **296,** 1648–1649
52. Aoyagi, K., and Takahashi, M. (2001) *Biochem. Biophys. Res. Commun.* **286,** 646–651
53. Osipenko, O. N., Barrie, A. P., Allen, J. M., and Gurney, A. M. (2000) *J. Biol. Chem.* **275,** 16626–16631
54. Taupenot, L., Ciesielski-Treska, J., Ulrich, G., Chasserot-Golaz, S., Aunis, D., and Bader, M. F. (1996) *Neuroscience* **72,** 377–389
55. Cavallaro, S., D'Agata, V., Guardabasso, V., Travali, S., Stivala, F., and Canonico, P. L. (1995) *Mol. Pharmacol.* **48,** 56–62
56. Ravni, A., Eiden, L. E., Vaudry, H., Gonzalez, B. J., and Vaudry, D. (2006) *J. Neurochem.* **98,** 1229–1241
57. Brandish, P. E., Su, M., Holder, D. J., Hodor, P., Szumiloski, J., Kleinhanz, R. R., Forbes, J. E., McWhorter, M. E., Duenwald, S. J., Parrish, M. L., Na, S., Liu, Y., Phillips, R. L., Renger, J. J., Sankaranarayanan, Simon, A. J., and Scolnick, E. M. (2005) *Neuron* **45,** 861–872
58. Wong, A. O., Li, W., Leung, C. Y., Huo, L., and Zhou, H. (2005) *Endocrinology* **146,** 5407–5424
59. Baldelli, P., Hernandez-Guijo, J. M., Carabelli, V., Novara, M., Cesetti, T., Andres-Mateos, E., Montiel, C., and Carbone, E. (2004) *Mol. Neurobiol.* **29,** 73–96
60. Carbone, E., Carabelli, V., Cesetti, T., Baldelli, P., Hernandez-Guijo, J. M., and Giusta, L. (2001) *Pflugers Arch.* **442,** 801–813
61. Dolphin, A. C. (2003) *Pharmacol. Rev.* **55,** 607–627
62. Marley, P. D. (2003) *Pharmacol. Ther.* **98,** 1–34
63. Wallace, D. J., Chen, C., and Marley, P. D. (2002) *J. Physiol.* **540,** 921–939
64. Shibuya, I., Noguchi, J., Tanaka, K., Harayama, N., Inoue, U., Kabashima, N., Ueta, Y., Hattori, Y., and Yamashita, H. (1998) *J. Neuroendocrinol.* **10,** 31–42
65. Dziema, H., and Obrietan, K. (2002) *J. Neurophysiol.* **88,** 1374–1386
66. Powelka, A. M., and Buckley, K. M. (2001) *FEBS Lett.* **501,** 47–50
67. Caumont, A. S., Vitale, N., Gensse, M., Galas, M. C., Casanova, J. E., and Bader, M. F. (2000) *J. Biol. Chem.* **275,** 15637–15644
68. Galas, M. C., Helms, J. B., Vitale, N., Thierse, D., Aunis, D., and Bader, M. F. (1997) *J. Biol. Chem.* **272,** 2788–2793
69. Qiagen, Inc. *RNeasy® Mini Handbook*, (2001) 3rd Ed., pp. 31–35, Qiagen Inc.
70. Motulsky, H. J., and Christopoulous, A. (2003) Fitting Models to Biological Data Using Linear and Nonlinear Regression. *A Practical Guide to Curve Fitting*, pp. 222–232, GraphPad Software, Inc., San Diego, CA